Clim. Past Discuss., 9, 5077–5122, 2013
www.clim-past-discuss.net/9/5077/2013/
doi:10.5194/cpd-9-5077-2013

Climate of the Past
Discussions
Open Access

Magnetostratigraphy of sediments from Lake El'gygytgyn ICDP Site 5011-1: paleomagnetic age constraints for the longest paleoclimate record from the continental Arctic

E. M. Haltia[1,*] **and N. R. Nowaczyk**[1]

[1]Helmholtz Centre Potsdam, GFZ German Research Centre for Geosciences, Section 5.2, Climate Dynamics and Landscape Evolution, Telegrafenberg, 14473 Potsdam, Germany
[*]now at: Department of Geography and Geology, Section of Geology, University of Turku, 20014 Turku, Finland

Received: 31 July 2013 – Accepted: 3 August 2013 – Published: 3 September 2013

Correspondence to: E. M. Haltia (eeva.haltia@utu.fi)

Published by Copernicus Publications on behalf of the European Geosciences Union.

Abstract

Paleomagnetic measurements were performed on sediments drilled from ICDP Site 5011-1 in Lake El'gygytgyn (67°30′ N, 172°05′ E) located in Far East Russian Arctic. The lake fills partly a crater formed by a meteorite impact 3.58 ± 0.04 Ma ago. Sediments from three parallel cores (5011-1A, 5011-1B and 5011-1C), recovered from the middle part of the lake, yielded a total of 355 m of sediment. Sediments are characterized by variable lithology, where intervals of homogenous and laminated sediments alternate, and mass movement deposits of variable thickness occur frequently along the sediment profile. Mineral magnetic investigation made on sediments enclosed in core catchers suggests that magnetic carrier in these sediments is partly maghemitized Ti-rich pseudo-single domain magnetite. Its detrital origin could be shown by mineral magnetic measurements and SEM-EDS analyses performed on mini-sized cylindrical rock samples, polished rock sections, creek sediments and magnetic extracts prepared from them. The intensity of the natural remanent magnetization (NRM) in the sediments is mainly high with a range from about 1 to 1000 mA m^{-1}. Most of the sediments carry a stable magnetization component interpreted as primary depositional remanent magnetization. Characteristic inclination data show alternating intervals of steep positive and negative inclinations that were used to assign magnetic polarity to the lake sediment profile. This was a rather straightforward procedure owing to the mainly high quality of data. The Matuyama/Gauss (2.608 Ma) and Brunhes/Matuyama (0.780 Ma) reversals were recognized in the sediments. Furthermore, during the Gauss chron the Mammoth and Kaena reversed subchrons, and during the Matuyama, the Olduvai and Jaramillo normal subchrons, as well as the Réunion and Cobb Mountain cryptochrons were identified. Sediment deposition rate is highest at the base of the sequence laid down in the beginning of Gauss chron, when deposition rate is approximately 44 cm kyr^{-1}. Sediment deposition decelerates upcore and it is an order of magnitude lower during the Brunhes chron when compared to that in early the Gauss chron. Decrease in sediment deposition in late Pliocene probably relates to atmospheric and

Discussion Paper | Discussion Paper | Discussion Paper | Discussion Paper |

oceanic reorganization heralding the onset of Quaternary climate change. The high-quality magnetostratigraphy reconstructed from Lake El'gygytgyn sediments provides 12 tie-points to pin down the age of the longest paleoclimate record from the continental Arctic.

1 Introduction

Due to the combination of climate feedback mechanisms related to sea ice and ice sheet albedo, climate in the northern high latitudes is particularly sensitive to seasonal and latitudinal insolation variations on orbital timescales (e.g. Kutzbach et al., 1991). Investigation of long-term climatic history in the continental Arctic has been hindered by a lack of data from high latitude depositional sites, where continuous sedimentary records extending beyond the termination of the last glacial would have been preserved. Obtaining a long and continuous climate record from an Arctic continental site is crucially important in an attempt to reconstruct the character and timing of climatic variability and its environmental response during the Quaternary, or even longer back in time. This would also enable establishing climatic teleconnections between records from different archives, such as lacustrine and marine sediments, ice cores, or loess, and add to the more comprehensive understanding of the functioning of the climatic system (Katz et al., 2011).

Pilot study of sediment core PG1351 recovered in 1998 from Lake El'gygytgyn, which occupies a meteorite impact crater in Far East Russian Arctic, revealed a continuous record of paleoenvironmental variability responding to orbitally driven summer insolation during the last 250 kyr (Brigham-Grette et al., 2007; Nowaczyk et al., 2007). Inferring from geomorphological analysis of end moraines deposited by valley glaciers and associated cosmogenic isotope dating, Far East Russia has not been covered by an ice-sheet at least since the Middle Pleistocene (Brigham-Grette et al., 2003). This renders the lake an attractive target for drilling a unique and temporally longest continental sediment sequence from the Arctic. This objective in prospect, deep drilling in Lake

CPD
9, 5077–5122, 2013

El'gygytgyn was executed within the framework of the ICDP (International Continental Scientific Drilling Project) Lake El'gygytgyn Drilling Project in spring 2009 (Melles et al., 2011). The significance of this unique and continuous paleoclimatic record, which extends into mid-Pliocene, is summarized by Melles et al. (2012) and Brigham-Grette et al. (2013). Developing an accurate sediment chronology is of key importance in unlocking the climatic record preserved in the sediments from El'gygytgyn. The capability of remanence-carrying iron oxides in sediments and rocks to record geomagnetic polarity variations enables their dating by matching the reconstructed magnetostratigraphic variations with respect to geomagnetic polarity timescales (e.g. Cande and Kent, 1995; Opdyke and Channell, 1996). This paper presents and discusses magnetostratigraphic results from this unique Arctic lake, which forms the principal chronological framework for the sediments recovered during the deep drilling of Lake El'gygytgyn. In order to obtain preliminary information about the carrier of paleomagnetic signal and its origin in these sediments, mineral magnetic properties of lake sediments and rock samples and sediments from the catchment were investigated.

2 Site description

Lake El'gygytgyn (67°30′ N, 172°05′ E; 492 m a.s.l.) is a crater lake located in the mountainous central Chukotka Peninsula in Far East Russian Arctic. According to most recent results from $^{40}Ar/^{39}Ar$ dating, the 18 km wide crater was formed as a result of a meteorite impact into mid-Cretaceous silicious volcanic rock series in the middle Pliocene at 3.58 ± 0.04 Ma (Layer, 2000). Dominant rock types include rhyolitic and dacitic tuffs, ignimbrites and lavas, and to a lesser extent, andesitic tuffs and lavas, which are overlain by basalts in the northeastern part of the crater rim (Gurov and Koeberl, 2004). The lake basin is bowl-shaped with steep flanks and a flat bottom, enclosing a lake with a diameter of 12 km, surface area of 110 km^2 and maximum depth of 175 m. The catchment (293 km^2) is small in relation to the lake surface area and, during summertime, its permafrost soils are drained by ca. 50 ephemeral creeks radially directed with

CPD
9, 5077–5122, 2013

E. M. Haltia and N. R. Nowaczyk

respect to the lake (Fig. 1). The lake has one outlet, the Enmyvaam River, which has cut its way through the crater rim in the southeast and drains into Bering Sea. Based on the interpretation of refraction- and reflection-seismic data, the layered sediment infill was estimated to have a thickness of 320 to 340 m (Gebhardt et al., 2006, 2013). This was confirmed by the ICDP drilling, hitting the transition zone from sediments to impact breccia at a depth of around 316 m. Currently, the lake is oligotrophic and monomictic, and the water column becomes thermally stratified under the ice cover, which persists from October to mid-July. The lake becomes thoroughly mixed by strong winds during the intervening ice-free months (Nolan and Brigham-Grette, 2007). Climate in the arctic Chukotka Peninsula is continental and according to weather data collected in 2002 the annual mean temperature was −10.3 °C with annual extreme values ranging from −40 to +26 °C (Nolan and Brigham-Grette, 2007). The sparse vegetation in the area is tundra dominated by herbs and low shrubs (Lozhkin et al., 2007).

3 Material and methods

3.1 Lake drilling and sediment core handling

As a result of a long-standing planning and international cooperation, sediments and underlying impact breccia were cored within the frame of the ICDP Lake El'gygytgyn Drilling Project from October 2008 to May 2009. Drilling operations and on-site processing of cores are documented in detail by Melles et al. (2011) and here they are only briefly reviewed. Coring was undertaken from an ice platform using Russian GLAD 800 drill rig, which is specially adapted for use in arctic conditions. Sediment cores were drilled from ICDP Site 5011-1 in the flat middle part of the lake (67°29.98′ N, 172°6.23′ E) from three parallel holes, 5011-1A, 5011-1B and 5011-1C (Table 1). For brevity, sediment cores from these holes will be referred to as cores 1A, 1B and 1C, respectively. The gradual transition from sediment to underlying impact breccia occurs approximately at 316 m below lake floor (Gebhardt et al., 2013). Coring tools were selected according to increasing sediment stiffness with depth, and hydraulic piston corers, non-rotating/rotating, and hard rock bit corers were employed. Rather long intervals in core 1C were hampered by incomplete sediment recovery (Table 1), which may be related to coarse sediment intervals encountered at this part of the sequence and/or the coring tool employed (Melles et al., 2011).

In the laboratory, sediment sections enclosed in liners were cut lengthwise with a circulating saw and subsequently the sediment was split into two halves (i.e. a working half and an archive half) using a nylon string. The consolidated sediments in the bottommost sections recovered from hole 1C were cut lengthwise in half with a circular saw. After opening, lithological description of the sediments was made and they were subjected to various non-destructive optical, magnetic, geochemical and physical analyses (Melles et al., 2011). Sediments were subsampled according to a predefined scheme with consistent aliquots for different types of analyses. A composite sediment record was reconstructed during core processing and subsampling of sediments from cores 1A, 1B and 1C, which included, among other things, identification of more than 300 mass movement deposits and their exclusion from the final paleoclimate record (Sauerbrey et al., 2013; Wennrich et al., 2013; Nowaczyk et al., 2013).

3.2 Paleomagnetic sampling and measurements

The majority of paleomagnetic measurements were made on working halves of sediment sections sampled in u-channels, 2×2 cm in cross section, either 110 or 75 cm in length, depending on sediment recovery in the individual sections. Paleomagnetic sampling was executed along the central part of the core sections to avoid sheared sediment adjacent to liner walls. Cores 1A and 1B were sampled solely using u-channels. The sediments from core 1C were mainly sampled using paleomagnetic sample boxes ($n = 446$; dimensions $2 \times 2 \times 1.5$ cm; volume ca. 6 cm^3) in the sediment interval extending from 141.8 to 311 m. Alternatively, u-channel samples were taken where possible. Discrete sampling was made by pushing a sediment sampler with a square cross section and internal dimensions of 1.9×1.9 cm into the sediment in

CPD
9, 5077–5122, 2013

E. M. Haltia and N. R. Nowaczyk

order to cut a cubical sample, which was then extruded into a paleomagnetic sample box. Discrete sampling was preferred because increasing sediment stiffness downcore hampered sampling in u-channels. Moreover, discrete sampling allowed targeting sampling to undisturbed clayey and silty sediments, which have more potential to yield reliable paleomagnetic data than coarser-grained sediments encountered in core 1C. Whenever possible, discrete samples were taken in steps of 10 cm. However, the actual sampling spacing is 12.6 cm due to the avoidance of sand layers and disturbed sediment sections. Sampling was continued until 311 m. From this depth downwards until 316 m sediment is highly consolidated gravel and pebbles in a sandy matrix and cutting paleomagnetic samples without disturbing the sediment was not possible. Then again, sediment was too brittle to be sampled using a rotating diamond drill bit. Therefore, a non-standard sampling technique was applied in order to obtain half-oriented samples with a known vertical orientation but unknown azimuth. In general, the half-cylindrical sediment columns of the archive halves were broken into segments (discs) of various length (thickness) by the coring process. The archive halves were placed directly next to the sample holder of the long-core magnetometer. Then, suitable sediment segments or discs were individually taken out of the liner for sub-sampling, and a non-magnetic saw blade was used to cut off approximately triangular, partly irregular pieces. The resulting samples, approximately 5 to 8 cm^3 in volume, were placed directly into the magnetometer's sample holder in order to avoid misorientation. The employed sample holder has been designed to take up eight cylindrical samples of 10 cm^3 that can be fixed by a plastic spring in order to avoid movement or rotation of the samples during measurements. Because the sediment pieces were fairly crumbly they were fitted back into the archive halves directly after measurement of the magnetization and no further magnetic investigation was performed on them.

Natural remanent magnetization (NRM) was measured from the paleomagnetic samples with a 2G Enterprises 755-SRM cryogenic long-core magnetometer. The NRM was progressively demagnetized in ten steps (5, 10, 15, 20, 30, 40, 50, 65, 80 and 100 mT) with the magnetometer's inline three-axis demagnetizer. The remaining NRM

CPD
9, 5077–5122, 2013

E. M. Haltia and N. R. Nowaczyk

was measured after each demagnetization step. The direction of the characteristic remanent magnetization (ChRM), i.e. the magnetization component interpreted to carry primary and supposedly syn-depositional information, was isolated using the progressively demagnetized NRM data from five to seven successive AF-demagnetization steps picked by the eye using principal component analysis (Kirschvink, 1980). The precision of ChRM determination is expressed by the maximum angular deviation (MAD). MAD values $\leq 5^{\circ}$ are interpreted to characterize samples where a single component magnetization has been isolated. The magnetometer's pick-up coils integrate data over about 9.5 cm. Thus, in order to eliminate spurious results due to edge effects, data collected along the upper and lower 4 cm of a u-channel were excluded from the final paleomagnetic data.

Unless otherwise is stated, ages for the polarity transitions are derived from LR04, which is a benthic foraminiferal oxygen isotope ($\delta^{18}O$) stack with a global distribution of the constituting data (Lisiecki and Raymo, 2005). LR04 is employed here, because the chronological framework provided by magnetic polarity reversals is further refined by tuning of different sedimentary paleoclimate proxies sensitive to climatic and insolation variations in orbital time scales with respect to the LR04 stack as a reference curve (Nowaczyk et al., 2013).

3.3 Mineral magnetic measurements on lake sediments

Investigation of mineral magnetic properties, i.e. the concentration, grain size, and mineralogy of magnetic minerals, is vital for identifying the carrier(s) of remanence in the sediment. Mineral magnetic parameters allow making inferences concerning the source and origin of magnetic minerals, their depositional environment, and diagenetic processes therein. In some cases, post-depositional diagenetic processes and/or growth of secondary authigenesis of magnetic minerals, such as the ferrimagnetic mineral greigite (Fe_3S_4), may have altered or even completely erased the primary NRM originating from the time of sediment deposition (Snowball, 1991; Dearing et al., 1998; Roberts and Weaver, 2005). Therefore, careful identification of carrier(s)

CPD
9, 5077–5122, 2013

E. M. Haltia and N. R. Nowaczyk

of remanence has important implications for consideration of the reliability of paleomagnetic dating. While sediments sampled in u-channels were considered as archival material, sediment enclosed in core catchers, one in every three meters of sediment, from the cores 1A to 1C was available for a mineral magnetic investigation. One sample was taken from each core catcher by pressing a paleomagnetic sample box (volume $6\,cm^3$) into the upper surface of the sediment block. Selected magnetic parameters were determined to estimate the concentration, mineralogy and magnetic grain size range of the carriers of remanence in these samples ($n = 122$). These parameters are listed together with their description and information on the instrumentation in Table 2. More information on mineral magnetic parameters and their interpretation can be found e.g. in Thompson and Oldfield (1986). After finalizing the magnetic measurements on bulk samples, samples were freeze-dried and gently ground with an agate mortar and pestle. Subsamples for magnetic hysteresis measurements were prepared by mixing ground sediment with a droplet of superglue and preparing $3 \times 3\,mm$ pellets ($n = 122$) for analysis.

3.4 Mineral magnetic measurements on catchment rocks and creek sediments

Besides the lacustrine sediments, catchment rocks and sediments collected from creeks draining the catchment were investigated to collect additional information on the source and origin of magnetic minerals in the sediments deposited in Lake El'gygytgyn. Rock samples were collected from the catchment during an expedition to the lake in spring 2003 (Melles et al., 2005). These samples were available for screening of mineral magnetic properties of the source rocks. Distribution of the analyzed rock samples within the catchment is not uniform, but approximately two thirds of the collected rock samples are from the area extending from east to southwest of the lake, and the remaining third originates from an area northwest of lake (Fig. 1). The uneven distribution of collected samples due to a lack of suitable outcrops introduces a spatial bias, but preliminary apprehension of the magnetic properties of the catchment rocks, appropriate for the purposes of this study, is acquired. Part of the rock samples ($n = 23$) were

CPD
9, 5077–5122, 2013

taken as oriented hand samples directly from available bedrock outcrops, whereas most of the samples were collected from periglacial colluvium ($n = 58$) from the foots of slopes surrounding the lake. Where necessary, these two sample types are jointly referred to as catchment rocks. Cylinder-shaped mini-sized specimens ($n = 80$; mean diameter 12 mm, volume 2.0 cm^3) were drilled from the catchment rock samples. Low-field magnetic volume susceptibility (κ_{LF}), complete stepwise acquisition of isothermal remanent magnetization (IRM), and the S-ratio were measured from the catchment rocks in a fashion identical to lake sediment samples (Table 2). Hysteresis measurements were not performed on catchment rock samples.

Bulk sediment samples from bedload of creeks and shallow lagoons, blocked by coarse sand bars in the mouth of creeks, were collected during the same expedition as the catchment rocks. From now on, these sediments are jointly referred here to as creek sediments. Creek sediments from 32 sites, distributed evenly across the lake circumference, were packed tightly in paleomagnetic sample boxes (6 cm^3) and stabilized by epoxy resin for measurements of mineral magnetic properties. In Table 2 more information is provided on magnetic measurements performed on creek sediments.

3.5 SEM-EDS analysis of magnetic separates from creek sediments

In order to investigate mineralogy and to visually characterize magnetic grains in more detail, magnetic minerals were investigated from polished rock sections and magnetic separates extracted from creek sediments. Magnetic minerals were manually separated from selected air-dried creek sediment samples using a rare earth magnet. Subsamples taken from these magnetic separates were mounted on standard SEM stubs and sputtered with carbon for inspection with a scanning electron microscopy (SEM), equipped with an energy dispersive X-ray spectroscopy facility (EDS), using a Zeiss Ultra 55 Plus. The instrument permits elemental analyses of the separated magnetic minerals and detailed observation of grain morphology. Magnetic minerals present in rocks were investigated from polished sections ($n = 19$, thickness 0.5 mm), which were

CPD
9, 5077–5122, 2013

prepared from the mini-sized specimens. The polished sections were glued onto glass slides, coated with carbon and analyzed with the SEM-EDS.

4 Results and interpretation

4.1 Polarity stratigraphy of cores 1A and 1B

NRM intensity is generally high and values range mainly between 1 and 100 $mA\,m^{-1}$ (Fig. 2). The sediments mostly display a strong and stable magnetization, which decreases in a monotonous fashion towards the origin. However, some samples showed two or more components of magnetization, and stable direction of magnetization was isolated after removal of low-stability components at AF demagnetization of 15 mT (Fig. 3). The interval most often applied in the determination of ChRM was that from 15 to 65 mT. The magnetization is mainly carried by magnetic minerals of low coercivity, and usually ≤ 5 % of the NRM remains after completion of the AF magnetic cleaning at 100 mT (Fig. 4). However, in a few cases, contribution from high-coercive minerals was evident, with 50 % of the NRM remaining after applying the peak demagnetizing field. In most cases MAD values are < 5°, which indicates that a well-defined magnetization was isolated during principal component analysis. However, MAD values would have been higher in those samples, which carry multiple components of magnetization, in case a standard interval for defining the ChRM inclination would have been applied uniformly. Samples with multiple components of magnetization are characterized by low NRM intensity and significant contribution of magnetically harder minerals and consequently their paleomagnetic value might be equivocal.

In cores 1A and 1B, characteristic inclination is usually revealed by the 15 mT demagnetization step. Only the inclination of the ChRM will be discussed here, because the sediment sections were oriented with respect to their z-axis, but azimuth angle is unknown. Inspection of ChRM inclination records from cores 1A and 1B revealed similar patterns of sediment intervals, which have mostly steep inclination with either

CPD
9, 5077–5122, 2013

Magnetostratigraphy of sediments from Lake El'gygytgyn

E. M. Haltia and N. R. Nowaczyk

normal or reversed polarity (Fig. 5), and normal polarity inclinations oscillate around the expected axial dipole inclination value of 78.3° for ICDP Site 5011-1. The reconstructed patterns of ChRM inclination from cores 1A and 1B can be readily correlated to the established pattern of magnetic field reversals during the last 2.6 Myr (Ogg and Smith, 2004), and polarity reversals in cores 1A and 1B, proceeding from top to down, are interpreted as follows. Polarity changes from normal to reversed down-core at 28 m is correlated to the Brunhes/Matuyama boundary at 0.780 Ma. In two sediment intervals within the Matuyama chron polarity is consistently normal. These sections extend from 38 to 40.5 m and from 75 to 84 m, and they are interpreted as the Jaramillo subchron (1.075 to 0.991 Ma) and the Olduvai subchron (from 1.968 to 1.781 Ma), respectively. The sediments from early Olduvai are recovered only in core 1B and they are characterized by scattered magnetization directions. However, data are partly unreliable because of complex folding structures overturning the sediment strata, which renders polarity reconstruction complex. During the Matuyama, two additional, short normal polarity intervals were identified in both cores. These are centered at 44 and 97 m, and they are interpreted as the Cobb Mountain cryptochron (Mankinen et al., 1978) (1.185 to 1.173 Ma) and the Réunion subchron (Chamalaun and McDougall, 1966) (from 2.148 to 2.128 Ma), respectively (ages from Ogg and Smith, 2004). Interestingly, both cores recorded a short interval of reversed polarity directions during the late Jaramillo subchron at 39 m, possibly correlative to the intra-Jaramillo excursion, which has been suggested to represent a global short geomagnetic excursion (Pillans et al., 1994; Channell and Kleiven, 2000). Another possible short geomagnetic event is detected at the depth of ∼ 85 m in both cores, with a "flip" to normal polarity just before the onset of the Olduvai subchron, which may represent the Olduvai precursor (1.977 Ma) (Channell et al., 2003). With an unfortunate coincidence with a core break, polarity shifts from normal to reversed at the sediment depth of 122 m in core 1A. This depth approximates the Matuyama/Gauss reversal, which occurred at 2.608 Ma.

In some sediment sections, such as that from 72 to 70 m in core 1A, ChRM inclinations are notably shallow and without a counterpart in the sediments in the parallel core.

CPD
9, 5077–5122, 2013

These represent either sediment disturbances and/or coarse-grained mass movement deposits, where paleomagnetic direction has been destroyed or poorly recorded. These are not taken as reflections of past geomagnetic field configurations.

4.2 Polarity stratigraphy of core 1C

The NRM intensity in core 1C is high and values range mainly between 10 and 1000 $mA\,m^{-1}$. Highest NRM values are found in the bottommost sediments of the core (Fig. 6). In general, the sediments display a strong and stable magnetization, as was the case in cores 1A and 1B (Fig. 3). Inspecting the reconstructed ChRM inclination record from core 1C (Fig. 6) in context with the paleomagnetic records from cores 1A (Fig. 5), the shift from reversed to normal polarity at 121.5 m can be assigned as the Matuyama/Gauss boundary, which coincided with a core break in core 1A. A more ambiguous paleomagnetic sequence, with a more scattered directional record with normal and reversed polarities arises from the sediments between 145 and 290 m, or between 2.95 and 3.55 Ma. This part of sediment sequence is characterized by higher sand and gravel content in comparison with younger sediments. Sediments between ca. 158 and 161.5 m show mainly reversed polarity, and this interval is interpreted to represent the Kaena subchron (3.127 to 3.045 Ma). Due to low quality of data, termination of Kaena remains vaguely determined in the paleomagnetic record. Below the Kaena, ChRM inclinations mainly have a normal polarity. Between 169.6 and 193.8 m sediments display again an interval with somewhat scattered polarities, but the polarity tends to stay more in reversed than normal mode. Thus, these sediments are interpreted to have been deposited during the Mammoth subchron (3.319 to 3.210 Ma). Unfortunately, there is a gap in sediment recovery directly below 193.8 m. Directly below this gap, the polarity is predominantly normal and represents the Gauss chron. As a consequence, the onset of Mammoth cannot be precisely determined from paleomagnetic data alone. Sediment intervals extending from 224 to 241.5 m and especially that from 280 to 286.5 m show several data points with reversed polarity sandwiched between those correlated to the early normal polarity Gauss. These cannot be correlated to any known and widely ac-

CPD
9, 5077–5122, 2013

cepted geomagnetic polarity events or excursions. The deeper parts of the sediment record (≥ 287 m) show continuously a normal polarity. These sediments can be interpreted to have been deposited during the early Gauss chron, bearing in mind that the crater was formed at 3.58 ± 0.04 Ma (Layer, 2000), shortly after the Gauss/Gilbert reversal (3.588 Ma).

4.3 Carrier of remanence in lake sediments and its origin

SEM-EDS microanalyses of polished sections revealed the ubiquitous presence of large multi-domain (MD) sized grains of titanium-substituted magnetite (Ti-magnetite, $Fe_{3-x}Ti_xO_4$), mainly between 10 and 100 µm in size, in catchment rocks (Fig. 7a). In many samples the Ti-magnetite grains are either uniformly finely fractured with irregular curved cracks, or alternatively they have a rim of fractures surrounding an apparently unaltered center. This fracturing is presumably caused by gradual low-temperature oxidation of Ti-magnetites, which results in outward migration of Fe-cations and relative enrichment of Ti-cations. This alteration process affecting magnetic properties is called maghemitization, which has been described from Ti-magnetites in volcanic rocks in different geological settings (Marshall and Cox, 1972; Akimoto et al., 1984; Cui et al., 1994; Nowaczyk, 2011). Besides maghemite (γ-Fe_2O_3, with a cation-deficient spinel structure), magnetite (Fe_3O_4) and spinels from the magnetite-chromite solid solution series ($FeFe_xCr_{2-x}O_4$; $0 \le x \le 2$) were detected. Hematite (α-Fe_2O_3, with a corundum structure) occurs often as narrow irregular veins (Fig. 7b), which fill in the spaces between other mineral crystals, or alternatively, as fine-grained inclusions in other minerals (Fig. 7b). In line with the results from polished rock sections, SEM-EDS analysis of some magnetic separates from creek sediments revealed Ti-magnetite grains in the large MD size range (Fig. 8a). In many cases, magnetite grains in El'gygytgyn hard rocks are associated with apatite intergrowths ($Ca_5(F,Cl,OH)(PO_4)_3$) (Figs. 7c and 8b). Similar to source rocks, many of the Ti-magnetite grains are cracked due to low-temperature oxidation of magnetic minerals. Some grains have notably rounded edges probably due to abrasion while being transported in creek bedload, but many particles

CPD
9, 5077–5122, 2013

E. M. Haltia and N. R. Nowaczyk

are characterized by an idiomorphic shape, or by sharp crystal edges, which indicates only short-distance transport from their source (Fig. 8c–e). Considering the small size of Lake El'gygytgyn catchment, sediment transport distances in creeks discharging into the lake can be expected to be short. While aeolian flux comprises today only a small part (2 %) of total sediment income in Lake El'gygytgyn (Fedorov et al., 2013), its role in transporting ferrimagnetic particles may have been more important during Pleistocene glaciations (Maher, 2011).

In accordance with results from microanalyses, results from mineral magnetic measurements suggest the dominance of low-coercivity minerals in the magnetic properties of catchment rocks, creek sediments and lake sediments. Results of the measured magnetic parameters including κ_{LF}, SIRM, S-ratio, SIRM/κ_{LF} and B_{CR}, are summarized in Table 3. Stepwise acquisition of IRM indicates that the majority of catchment rock samples and creek sediments acquired 90 % of their SIRM after application of a magnetic field ≤ 200 mT in strength (Fig. 9). Rapid acquisition of remanence in low magnetic fields (< 50 mT) supports the interpretation of a low-coercivity magnetic component, such as MD sized Ti-magnetite, as the dominating magnetic mineral in catchment rocks. High S-ratios measured from catchment rocks and creek sediments point again that Ti-magnetite is dominating their magnetic properties (Table 3). Concentration of magnetic minerals in catchment rocks, as estimated by SIRM and κ_{LF}, is comparable to that generally found in igneous rocks (Hunt et al., 1995). Expressed in terms of mass percentage using an average value of mass-specific susceptibility for Ti-magnetite of 422 $m^3\,kg^{-1}$ (SI 10^{-6}) (Peters and Dekkers, 2003), the mean concentration of Ti-magnetite in the source rocks can be estimated as 0.96 %, with a range from 0.01 to 4.15 %. The variable lithology and the variable degree of physical and chemical alteration of the investigated source rocks is reflected in the highly variable concentration of magnetic minerals in the analyzed rock samples, and it is also characterized by κ_{LF} vs. SIRM bi-plot, which visualizes variations in the mineralogy, concentration, and grain size of magnetic minerals (Fig. 10). Colluvial rock samples yield higher but less clustered SIRM values (Table 3) in comparison with those samples drilled directly from

CPD
9, 5077–5122, 2013

bedrock (Fig. 10). This is tentatively interpreted to reflect a higher degree of maghemitization of Ti-magnetites in colluvium due to increased fracturing as a result of more efficient physical and chemical weathering compared to bedrock. Smaller magnetite grains are more efficient to acquire and withhold remanence, which might explain the higher SIRM values in colluvium.

Hematite appears to be absent in creek sediments and consequently the magnetic mineralogy seems to be more uniform in comparison to catchment rocks. Hysteresis properties presented in a Day plot (Day et al., 1977) show that the magnetic grain size of creek sediments lies in the region representing coarser pseudo-single domain range (Fig. 11). This is not directly in line with observation of large MD Ti-magnetite grains witnessed in SEM imaging, which could possibly be explained by alteration of magnetic properties due to maghemitization and associated shrinkage cracks, dividing large grains at least superficially, if not internally, into smaller domains. In their investigation of low-temperature oxidation on MD magnetite extracted from natural river sediments, Cui et al. (1994) concluded that the apparent decrease in magnetic domain state to PSD was due to (i) gradual maghemization of the original magnetite crystal, where the intact core is surrounded by a maghemite rim, (ii) internal stress in a composite grain, which contains an inner Ti-magnetite core and outer shell of maghemite, which increases wall energy and impedes addition of walls for a given grain size, and (iii) the presence of single-domain maghemite and MD magnetite being summed up as PSD behaviour. Some, or all of these alternatives could lead to the observed PSD behaviour of magnetic minerals in creek sediments in the catchment of Lake El'gygytgyn.

Creek sediments appear notably clustered in the SIRM vs. κ_{LF} bi-plot, and in that respect, they differ from the catchment rocks. Magnetic concentration in the creek sediments is lower compared to that in catchment rocks (Table 3), but their magnetic mineralogy and grain size are largely homogenous. Interestingly, magnetic grain size, as deduced from the ratio SIRM/κ_{LF}, appears larger in creek sediments than in catchment rocks. It is possible that the ratio does not respond sensitively to magnetic grain size in this case, where magnetic mineralogy is characterized by maghemitized Ti-magnetites.

CPD
9, 5077–5122, 2013

E. M. Haltia and N. R. Nowaczyk

In their review aiming to define the room-temperature magnetic parameters best characterizing different iron oxides and iron sulfides, Peters and Dekkers (2003) showed that κ_{LF} and SIRM values of maghemite is largely independent of grain size from PSD ($\sim$ 1–2 µm) to large MD ($\sim$ 200 µm), which explains, in this case, the insensitivity of the ratio SIRM/κ_{LF} to magnetic grain size variations.

Lake sediments acquire IRM in a manner similar to creek sediments (Fig. 9). However, approximately a quarter of samples indicate more pronounced contributions from magnetic minerals with harder coercivity, most likely hematite. This is also visible in the higher coercivity (B_{CR}) of lake sediments in comparison with creek sediments (Table 3). As discussed earlier, acquisition of IRM (Fig. 9) and SEM/EDS analysis (Fig. 7) indicated that catchment rocks contained some hematite. The difference between creek sediments and lake sediments may be explainable by hydrodynamic sorting. Possibly, hematite grains occur as inclusions in lighter minerals, which are selectively washed away from the creek bedload and deposited at the lake floor, concentrating the large maghemitized Ti-magnetite grains in creek sediments. Overlapping values in the Day plot (Fig. 11) indicate that lake sediments have a corresponding magnetic grain size distribution to that of creek sediments (Fig. 10). In the light of the linear relationship in the bi-plot SIRM vs. κ_{LF}, magnetic properties of lake sediments appear rather uniform over the whole sediment column, with concentration of magnetic minerals being higher in Pliocene sediments compared to those in Pleistocene sediments. However, as shown by Nowaczyk et al. (2007) and Murdock et al. (2013) using pilot cores from Lake El'gygytgyn, the concentration of magnetite in sediments is mainly controlled by the hypolimnetic redox conditions through large-scale magnetite dissolution during glacials and not simply by detrital input. Moreover, vivianite ($Fe_3(PO_4)_2 * 8H_2O$) nodules with relatively high susceptibility (mean value $1.05 \times 10^{-6}\ m^3\,kg^{-1}$) are present in sediments deposited during warm and cold climate stages (Minyuk et al., 2013), which may complicate paleoenvironmental interpretation of magnetic susceptibility in terms of paleoclimate, where cold intervals are characterized by low magnetic susceptibility. Thus, it is not possible to infer paleoenvironmental implications from mineral magnetic parameters alone. As shown by Frank et al. (2013) using pilot cores from Lake El'gygytgyn, statistical analysis of biochemical, inorganic and mineral magnetic data provides a more complete understanding of paleoenvironmental changes when refining the pattern of different climate modes in the sediments.

5 Discussion

Magnetic polarity stratigraphy reconstructed from the sediments from cores 1A and 1B from Lake El'gygytgyn compares favorably to the acknowledged frame of geomagnetic polarity changes starting from the early Gauss chron to late Brunhes. The directional stability of the sediments, with partly maghemitized detrital PSD-sized Ti-magnetite as the carrier of magnetization, enables reliable reconstruction of geomagnetic field changes from the sediments. The successful reconstruction of geomagnetic field changes during the Pleistocene and late Pliocene epochs comprises the main framework of geochronology for the sediments and enables pinning down the age of fixed horizons along the sediment profile. These magnetostratigraphic tie points form the chronological frame for aligning (tuning) the different sediment climate proxy parameters with respect to orbital changes, which refines the temporal resolution of the sediment chronostratigraphy (Nowaczyk et al., 2013). The paleomagnetic composite record, amalgamated using data from cores 1A, 1B, and 1C, is shown in Fig. 12. Composite depth values for polarity reversals and their respective ages are given in Table 4.

In comparison with the characteristic inclination records from cores 1A and 1B, which extend as far as 2.9 Myr back in time, most of the polarity record from hole 1C is rather noisy with the exception of sediments deposited during early and late Gauss chron, when polarity is mainly normal (Fig. 6). There are several factors, which can contribute to the noisier inclination record in core 1C. Unlike cores 1A and 1B, most of the sediment record covered by the core 1C does not have a duplicate. Technical problems during drilling of core 1C lead to incomplete sediment recovery (Melles et al., 2011). Moreover, extensive parts of the late Pliocene sediments are characterized by sandy and gravelly layers, which are not ideal for recording geomagnetic field changes. Discrete samples yield point data, which may produce a noisy inclination record if, for example, the sampled sediment displays low NRM intensity, or there are localized but unnoticed disturbances in the sediment. By comparison, paleomagnetic measurements from u-channels integrate data over sediment intervals ~ 10 cm in length, which results in low-pass filtering of the paleomagnetic data, whereby localized disturbances do not stand out as much from the data (Roberts, 2006).

Nevertheless, the magnetostratigraphic interpretation regarding placing the onset of Mammoth subchron in the paleomagnetic record in core 1C is supported by paleoenvironmental proxy data. Interpretation of results from pollen analysis (Tarasov et al., 2013) supports the chronological constrains set by magnetostratigraphy. Coinciding with the anticipated early Mammoth subchron, pollen data indicate a change in the paleoenvironment of Lake El'gygytgyn into cold and drought tolerant climate regime with steppe vegetation. Marine isotope stage (MIS) M2 occurs in the early Mammoth subchron, and in previous studies MIS M2 has been connected with a global cooling event and an increase in ice volume (Dwyer and Chandler, 2009; Schepper et al., 2009). In consequence, the occurrence of plant taxa indicating cooler climate at about 3.3 Ma in core 1C is interpreted to be coeval with MIS M2, and thus supports the interpretation of magnetostratigraphic data from Lake El'gygytgyn.

The completeness of the ICDP Site 5011-1 magnetostratigraphic record (Fig. 12), which shows all the widely acknowledged magnetic polarity chrons, subchrons, and even cryptochrons such as Réunion and Cobb Mountain, attests to the absence of any major hiatuses in the sediment record. This adds to the debate of the glacial history of Western Beringia and to the evidence presented by Brigham-Grette et al. (2003) in support of an ice-sheet free Far East Russia since the Middle Pleistocene.

Using the present paleomagnetic approach, the age of the El'gygytgyn impact structure can be loosely bracketed between the onset of Mammoth subchron at 3.319 Ma onset of Gauss chron, for which Ogg and Smith (2004) place at 3.588 Ma. In the base of the sequence at ICDP Site 5011-1, sediments show a consistently normal polar-

CPD
9, 5077–5122, 2013

Magnetostratigraphy of sediments from Lake El'gygytgyn

E. M. Haltia and N. R. Nowaczyk

ity, which suggests that these sediments are definitely younger than the Gauss/Gilbert polarity reversal (3.588 Ma). The most recent $^{40}Ar/^{39}Ar$ dating results placed the timing of the asteroid impact forming the El'gygytgyn crater at 3.58 ± 0.04 Ma ago (Layer, 2000). Previous work using fission track dating placed the corrected age estimate of the structure at 4.52 ± 0.11 Ma (Storzer and Wagner, 1979). An even older result from K/Ar dating was proposed by Belyi (1998), who suggested that volcanic activity in the area between 5.8 ± 0.5 Ma and 8.4 ± 0.7 Ma would have given rise to the structure. In the light of first-time paleomagnetic results from the present study, the results both from fission track and K/Ar dating can be taken as inaccurate, and it can be concluded that results from $^{40}Ar/^{39}Ar$ dating (Layer, 2000) give presently the most accurate estimate of the age of the impact.

Using the magnetic polarity chronology, general variations in sediment deposition rate from late Pliocene to late Pleistocene can be outlined. In the early history of the crater, in the time period between the impact at 3.58 ± 0.04 Ma (Layer, 2000) and the onset of the Mammoth subchron at 3.319 Ma, the mean sedimentation rate was an order of magnitude higher (∼ 44 cm kyr^{-1}) compared to the sediments accumulated since the beginning of the Pleistocene and until the the most recent part of the record (Fig. 13). Early and Middle Pliocene climate in the Arctic was warmer and moister than present (Salzmann et al., 2011), as characterized, for example, by the presence of boreal forests on Ellesmere Island (Ballantyne et al., 2006). Moister Pliocene climate can be postulated to have promoted fluvial supply of detrital matter from the lake catchment to the basin, as witnessed in the higher sedimentation rates in comparison with those reconstructed for the Pleistocene. The shift from Pliocene to Pleistocene, in general, is associated with reorganization of atmospheric and oceanic circulation patterns, leading to global paleoenvironmental changes, as evidenced, for example, by the formation of Northern Hemisphere ice sheets (Raymo, 1994) and large-scale aridification in the subtropical latitudes on both hemispheres (deMenocal, 2004; McLaren and Wallace, 2010). Therefore, the deceleration of sedimentation in Lake El'gygytgyn relates to the reorganization of atmospheric circulation over the circumpolar area through changes

CPD
9, 5077–5122, 2013

in surface hydrologic processes, decreasing thickness of soil active layer and formation of permafrost and thus it reflects in part the sensitivity of the El'gygytgyn sedimentary record to climatic change (Schwamborn et al., 2012). However, the high sedimentation rates, which fill in the basin rapidly in the early history of the crater, are probably also promoted by geological processes. The newly formed outer crater rim structure with unstable steep inner flanks, which rose up to 230 m above the present lake level, provided abundant erodible clastic material (Gurov and Koeberl, 2004), increasing the flux of clastic material into the lake. During late Quaternary, lake water table changes have followed climatic variability with higher levels inferred to have occurred during warmer periods (Juschus et al., 2011). Anticipated high water tables during Pliocene times likely promoted the input of detrital matter from the catchment by enhanced wave action in the first ~ 200 kyr since the crater formation. During this time, sediment deposition rate is at its highest. After this initial stage in sediment deposition in Lake El'gygytgyn the sedimentation slows down significantly.

Lower sedimentation rates during the Pleistocene probably prolonged the magnetization lock-in time in Lake El'gygytgyn sediments and thus decreased temporal resolution of the obtained paleomagnetic data. This might be the reason why most of the geomagnetic excursions documented to have taken place during the Matuyama and Brunhes chrons (Laj and Channell, 2009) are missing in the ICDP Site 5011-1 record. In addition to low sedimentation rates, the position of Lake El'gygytgyn may decrease the probability of very short-term geomagnetic changes of being recorded, because polarity change is anticipated to take a longer time at high latitude sites compared to lower latitudes (Clement, 2004). However, the presence of Olduvai precursor and Intra-Jaramillo excursions, lasting only 3.3 and 5 kyr, respectively, Nowaczyk et al. (2013) suggests that even higher frequency variations in geomagnetic field can be recorded in favorable conditions in high latitude sites. The more scattered inclination record, and less clear-cut polarity boundaries during Pliocene in comparison with those in Pleistocene may also be due to higher sedimentation rates during Pliocene, which allow

CPD
9, 5077–5122, 2013

a more detailed recording of the transitional geomagnetic field configuration during reversals.

6 Conclusions

Sediment cores recovered from the three holes 1A, 1B, and 1C from ICDP Site 5011-1 in Lake El'gygytgyn, Far East Russian Arctic, provide a reliable record of geomagnetic polarity variations during the last approximately 3.58 Myr. Remanence is carried by partly maghemitized titanomagnetite, accompanied by some hematite, derived from the lake catchment and transported by numerous creeks discharging into the lake. Magnetostratigraphy of the sediments provide a total of 18 reversal horizons to pin down the sediment chronostratigraphy of the longest sediment record from the continental Arctic. In the base of the record, sedimentation rate is an order of magnitude higher (44.5 $\mathrm{cm\,kyr^{-1}}$) compared to sediments deposited during the Pleistocene. Deceleration of sedimentation rate is interpreted to respond to hydrological changes associated with Quaternary climate cooling and geological development of the crater structure. This magnetostratigraphic study rules out the incidence of the impact forming El'gygytgyn meteorite crater prior to the early Gauss chron.

Acknowledgements. We would like to thank the participants in the lake drilling campaign in 2008/2009 for recovering the long sediment cores from Lake El'gygytgyn. We are grateful to O. Juschus and G. Schwamborn for providing sample material from the El'gygytgyn catchment. We are grateful to G. Arnold for preparing the polished rock sections. H. Kemnitz and J. Herwig are acknowledged for their technical assistance at the SEM/EDS facility. The team of student assistants at the Department of Geology, University of Cologne, are thanked for paleomagnetic sampling of sediments in u-channels. R. Gromig is acknowledged for participating in the time-consuming task of paleomagnetic sampling using discrete paleomagnetic boxes. D. Ulbricht, G. Schwamborn and V. Wennrich are thanked for transporting u-channel samples from Cologne. Funding for this research was provided by the International Continental Scientific Drilling Program (ICDP), the US National Science Foundation (NSF), the German Federal Ministry of Education and Research (BMBF), Alfred Wegener Institute (AWI)

CPD
9, 5077–5122, 2013

Magnetostratigraphy of sediments from Lake El'gygytgyn

E. M. Haltia and N. R. Nowaczyk

and GeoForschungsZentrum Potsdam (GFZ), the Russian Academy of Sciences Far East Branch (RAS FEB), the Russian Foundation for Basic Research (RFBR), and the Austrian Federal Ministry of Science and Research (BMWF). The Russian GLAD800 drilling system was developed and operated by DOSECC Inc., the down hole logging was performed by the ICDP-OSG, and LacCore, at the University of Minnesota, handled core curation.

The service charges for this open access publication have been covered by a Research Centre of the Helmholtz Association.

References

Akimoto, T., Kinoshita, H., and Furuta, T.: Electron probe microanalysis study on processes of low- temperature oxidation of titanomagnetite, Earth Planet. Sc. Lett., 71, 263–278, 1984.

Ballantyne, A. P., Rybczynski, N., Baker, P. A., Harington, C. R., and White, D.: Pliocene Arctic temperature constraints from the growth rings and isotopic composition of fossil larch, Palaeogeogr. Palaeocl., 242, 188–200, 2006.

Belyi, V. F.: Impactogenesis and volcanism of the El'gygytgyn depression, Petrology, 6, 86–99, 1998.

Brigham-Grette, J., Gualtieri, L. M., Glushkova, O. Y., Hamilton, T. D., Mostoller, D., and Kotov, A.: Chlorine-36 and ^{14}C chronology support a limited last glacial maximum across central chukotka, northeastern Siberia, and no Beringian ice sheet, Quaternary Res., 59, 386–398, 2003.

Brigham-Grette, J., Melles, M., Minyuk, P., and Scientific Party: Overview and significance of a 250 ka paleoclimate record from El'gygytgyn Crater Lake, NE Russia, J. Paleolimnol., 37, 1–16, 2007.

Brigham-Grette, J., Melles, M., Minyuk, P., Andreev, A., Tarasov, P., DeConto, R., Koenig, S., Nowaczyk, N., Wennrich, V., Rosén, P., Haltia-Hovi, E., Cook, T., Gebhardt, C., Meyer-Jacob, C., Snyder, J., and Herzschuh, U.: Pliocene warmth, polar amplification, and stepped Pleistocene cooling recorded in NE Arctic Russia, Science, 340, 1421–1427, 2013.

Cande, S. C. and Kent, D. V.: Revised calibration of the geomagnetic polarity timescale for the Late Cretaceous and Cenozoic, J. Geophys. Res., 100, 6093–6095, 1995.

Chamalaun, F. H. and McDougall, I.: Dating geomagnetic polarity epochs in Réunion, Nature, 210, 1212–1214, 1966.
Channell, J. E. T. and Kleiven, H. F.: Geomagnetic palaeointensities and astrochronological ages for the Matuyama–Brunhes boundary and the boundaries of the Jaramillo Subchron: palaeomagnetic and oxygen isotope records from ODP Site 983, Philos. T. Roy. Soc. A, 358, 1027–1047, 2000.
Channell, J. E. T., Labs, J., and Raymo, M. E.: The Réunion Subchronozone at ODP Site 981 (Feni Drift, North Atlantic), Earth Planet. Sc. Lett., 215, 1–12, 2003.
Clement, B. M.: Dependence of the duration of geomagnetic polarity reversals on site latitude, Nature, 428, 637–640, 2004.
Cui, Y., Verosub, K. L., and Roberts, A. P.: The effect of low-temperature oxidation on large multi-domain magnetite, Geophys. Res. Lett., 21, 757–760, 1994.
Day, R., Fuller, M., and Schmidt, V. A.: Hysteresis properties of titanomagnetites: grain-size and compositional dependence, Phys. Earth Planet. Int., 13, 260–267, 1977.
Dearing, J. A., Boyle, J. F., Appleby, P. G., Mackay, A. W., and Flower, R. J.: Magnetic properties of recent sediments in Lake Baikal, Siberia, J. Paleolimnol., 20, 163–173, 1998.
deMenocal, P. B.: African climate change and faunal evolution during the Pliocene-Pleistocene, Earth Planet. Sc. Lett., 220, 3–24, 2004.
Dunlop, D. J.: Theory and application of the Day plot (M_{rs}/M_s vs. H_{cr}/H_c), 1. Theoretical curves and tests using titanomagnetite data, J. Geophys. Res., 107, 2056, doi:10.1029/2001JB000486, 2002.
Dwyer, G. S. and Chandler, M. A.: Mid-Pliocene sea level and continental ice volume based on coupled benthic Mg / Ca palaeotemperatures and oxygen isotopes, Philos. T. Roy. Soc. A, 367, 157–168, 2009.
Fedorov, G., Nolan, M., Brigham-Grette, J., Bolshiyanov, D., Schwamborn, G., and Juschus, O.: Preliminary estimation of Lake El'gygytgyn water balance and sediment income, Clim. Past, 9, 1455–1465, doi:10.5194/cp-9-1455-2013, 2013.
Frank, U., Nowaczyk, N. R., Minyuk, P., Vogel, H., Rosén, P., and Melles, M.: A 350 ka record of climate change from Lake El'gygytgyn, Far East Russian Arctic: refining the pattern of climate modes by means of cluster analysis, Clim. Past, 9, 1559–1569, doi:10.5194/cp-9-1559-2013, 2013.
Gebhardt, A. C., Niessen, F., and Kopsch, C.: Central ring structure identified in one of the world's best-preserved impact craters, Geology, 34, 145–148, 2006.

CPD
9, 5077–5122, 2013

E. M. Haltia and N. R. Nowaczyk

Gebhardt, A. C., Francke, A., Kück, J., Sauerbrey, M., Niessen, F., Wennrich, V., and Melles, M.: Petrophysical characterization of the lacustrine sediment succession drilled in Lake El'gygytgyn, Far East Russian Arctic, Clim. Past, 9, 1933–1947, doi:10.5194/cp-9-1933-2013, 2013.
Gurov, E. P. and Koeberl, C.: Shocked rocks and impact glasses from the El'gygytgyn impact structure, Russia, Meteorit. Planet. Sci., 39, 1495–1508, 2004.
Hunt, C. P., Moskowitz, B. M., and Banerjee, S. K.: Magnetic Properties of Rocks and Minerals, in: Rock Physics & Phase Relations: A Handbook of Physical Constants, edited by: Ahrens, T. J., AGU Ref. Shelf, vol. 3, AGU, Washington, D.C., 189–204, 1995.
Juschus, O., Pavlov, M., Schwamborn, G., Preusser, F., Fedorov, G., and Melles, M.: Late Quaternary lake-level changes of Lake El'gygytgyn, NE Siberia, Quaternary Res., 76, 441–451, 2011.
Katz, S. L., Hampton, S. E., Izmest'eva, L. R., and Moore, M. V.: Influence of long-distance climate teleconnection on seasonality of water temperature in the world's largest lake – Lake Baikal, Siberia, PLoS one, 6, e14688, doi:10.1371/journal.pone.0014688, 2011.
Kirschvink, J. L.: The least-squares line and plane and the analysis of palaeomagnetic data, Geophys. J. Int., 62, 699–718, 1980.
Kutzbach, J. E., Gallimore, R. G., and Guetter, P. J.: Sensitivity experiments on the effect of orbitally-caused insolation changes on the interglacial climate of high northern latitudes, Quatern. Int., 10–12, 223–229, 1991.
Laj, C. and Channell, J. E. T.: 5.10 Geomagnetic Excursions, in: Geomagnetism, Treatise on Geophysics, edited by: Kono, M., Elsevier, the Netherlands, 373–416, 2009.
Layer, P. W.: Argon-40/argon-39 age of the El'gygytgyn impact event, Chukotka, Russia, Meteor. Planet. Sci., 35, 591–600, 2000.
Lisiecki, L. E. and Raymo, M. E.: A Pliocene-Pleistocene stack of 57 globally distributed benthic δO records, Paleoceanography, 20, PA1003, doi:10.1029/2004PA001071, 2005.
Lozhkin, A., Anderson, P., Matrosova, T., and Minyuk, P.: The pollen record from El'gygytgyn Lake: implications for vegetation and climate histories of northern Chukotka since the late middle Pleistocene, J. Paleolimnol., 37, 135–153, 2007.
Maher, B. A.: The magnetic properties of Quaternary aeolian dusts and sediments, and their palaeoclimatic significance, Aeol. Res., 3, 87–144, 2011.

CPD
9, 5077–5122, 2013

E. M. Haltia and N. R. Nowaczyk

Mankinen, E. A., Donnelly, J. M., and Grommé, C. S.: Geomagnetic polarity event recorded at 1.1 My. B. P. on Cobb Mountain, Clear Lake Volcanic Field, California, Geology, 6, 653–656, 1978.
Marshall, M. and Cox, A.: Magnetic changes in pillow basalt due to sea floor weathering, J. Geophys. Res., 77, 6459–6469, 1972.
McLaren, S. and Wallace, M. W.: Plio-Pleistocene climate change and the onset of aridity in southeastern Australia, Global Planet. Change, 71, 55–72, 2010.
Melles, M., Minyuk, P., Brigham-Grette, J., and Juschus, O. (Eds.): The Expedition El'gygytgyn Lake 2003 (Siberian Arctic), Ber. Polarforsch. Meeresforsch., 509, 139 pp., 2005.
Melles, M., Brigham-Grette, J., Minyuk, P., Koeberl, C., Andreev, A., Cook, T., Fedorov, G., Gebhardt, C., Haltia-Hovi, E., Kukkonen, M., Nowaczyk, N., Schwamborn, G., Wennrich, V., and El'gygytgyn Scientific Party: The Lake El'gygytgyn scientific drilling project – conquering Arctic challenges through continental drilling, Sci. Drill. 11, 29–40, 2011.
Melles, M., Brigham-Grette, J., Minyuk, P. S., Nowaczyk, N. R., Wennrich, V., DeConto, R. M., Anderson, P. M., Andreev, A. A., Coletti, A., Cook, T. L., Haltia-Hovi, E., Kukkonen, M., Lozhkin, A. V., Rosén, P., Tarasov, P., Vogel, H., and Wagner, B.: 2.8 Million years of Arctic climate change from Lake El'gygytgyn, NE Russia, Science, 337, 315–320, 2012.
Minyuk, P. S., Subbotnikova, T. V., Brown, L. L., and Murdock, K. J.: High-temperature thermomagnetic properties of vivianite nodules, Lake El'gygytgyn, Northeast Russia, Clim. Past, 9, 433–446, doi:10.5194/cp-9-433-2013, 2013.
Murdock, K. J., Wilkie, K., and Brown, L. L.: Rock magnetic properties, magnetic susceptibility, and organic geochemistry comparison in core LZ1029-7 Lake El'gygytgyn, Russia Far East, Clim. Past, 9, 467–479, doi:10.5194/cp-9-467-2013, 2013.
Nolan, M. and Brigham-Grette, J.: Basic hydrology, limnology, and meteorology of modern Lake El'gygytgyn, Siberia, J. Paleolimnol., 37, 17–35, 2007.
Nowaczyk, N. R.: Dissolution of titanomagnetite and sulphidization in sediments from Lake Kinneret, Israel, Geophys. J. Int., 187, 34–44, 2011.
Nowaczyk, N. R., Melles, M., and Minyuk, P.: A revised age model for core PG1351 from Lake El'gygytgyn, Chukotka, based on magnetic susceptibility variations tuned to Northern Hemisphere insolation variations, J. Paleolimnol., 37, 65–76, 2007.
Nowaczyk, N. R., Haltia, E. M., Ulbricht, D., Wennrich, V., Sauerbrey, M. A., Rosén, P., Vogel, H., Francke, A., Meyer-Jacob, C., Andreev, A. A., and Lozhkin, A. V.: Chronology of Lake

El'gygytgyn sediments, Clim. Past Discuss., 9, 3061–3102, doi:10.5194/cpd-9-3061-2013, 2013.
Ogg, J. G. and Smith, A. G.: The geomagnetic polarity time scale, in: A Geologic Time Scale 2004, edited by: Gradstein, F. M., Ogg, J. G., and Smith, A. G., Cambridge University Press, Cambridge, 2004.
Opdyke, N. D. and Channell, J. E. T. (Eds): Magnetic Stratigraphy, International Geophysics Series, vol. 64, 341 pp., 1996.
Parry, L. G.: Shape-related factors in the magnetization of immobilized magnetite particles, Phys. Earth Planet. Int., 22, 144–154, 1980.
Peters, C. and Dekkers, M. J.: Selected room temperature magnetic parameters as a function of mineralogy, concentration and grain size, Phys. Chem. Earth, 28, 659–667, 2003.
Pillans, B. J., Roberts, A. P., Wilson, G. S., Abbott, S. T., and Alloway, B. V.: Magnetostratigraphic, lithostratigraphic and tephrostratigraphic constraints on Lower and Middle Pleistocene sea-level changes, Wanganui Basin, New Zealand, Earth Planet. Sc. Lett., 121, 81–98, 1994.
Raymo, M. E.: The initiation of Northern Hemisphere glaciation, Annu. Rev. Earth Pl. Sc., 22, 353–383, 1994.
Roberts, A. P.: High-resolution magnetic analysis of sediment cores: strengths, limitations and strategies for maximizing the value of long-core magnetic data, Phys. Earth Planet. Int., 156, 162–178, 2006.
Roberts, A. P. and Weaver, R.: Multiple mechanisms of remagnetization involving sedimentary greigite (Fe_3S_4), Earth Planet. Sc. Lett., 231, 263–277, 2005.
Salzmann, U., Williams, M., Haywood, A. M., Johnson, A. L. A., Kender, S., and Zalasiewicz, J.: Climate and environment of a Pliocene warm world, Palaeogeogr. Palaeocl., 309, 1–8, 2011.
Sauerbrey, M. A., Juschus, O., Gebhardt, A. C., Wennrich, V., Nowaczyk, N. R., and Melles, M.: Mass movement deposits in the 3.6 Ma sediment record of Lake El'gygytgyn, Far East Russian Arctic, Clim. Past, 9, 1949–1967, doi:10.5194/cp-9-1949-2013, 2013.
Schepper, S. D., Head, M. J., and Groeneveld, J.: North Atlantic Current variability through marine isotope stage M2 (circa 3.3 Ma) during the mid-Pliocene, Paleoceanography, 24, PA4206, doi:10.1029/2008PA001725, 2009.
Schwamborn, G., Fedorov, G., Ostanin, N., Schirrmeister, L., Andreev, A., and the El'gygytgyn Scientific Party: Depositional dynamics in the El'gygytgyn Crater margin: implications for the 3.6 Ma old sediment archive, Clim. Past, 8, 1897–1911, doi:10.5194/cp-8-1897-2012, 2012.

CPD
9, 5077–5122, 2013

Snowball, I. F.: Magnetic hysteresis properties of greigite (Fe_3S_4) and a new occurrence in Holocene sediments from Swedish Lappland, Phys. Earth Planet. Int., 68, 32–40, 1991.

Storzer, D. and Wagner, G. A.: Fission track dating of Elgygytgyn, Popigai and Zhamanshin impact craters: no sources for Australasian or North-American tektites, Meteoritics, 14, 541–542, 1979.

Tarasov, P. E., Andreev, A. A., Anderson, P. M., Lozhkin, A. V., Haltia, E., Nowaczyk, N. R., Wennrich, V., Brigham-Grette, J., and Melles, M.: The biome reconstruction approach as a tool for interpretation of past vegetation and climate changes: application to modern and fossil pollen data from Lake El'gygytgyn, Far East Russian Arctic, Clim. Past Discuss., 9, 3449–3487, doi:10.5194/cpd-9-3449-2013, 2013.

Thompson, R. and Oldfield, F.: Environmental Magnetism, Allen and Unwin, Great Britain, 227 pp., 1986.

Wennrich, V., Minyuk, P., Borkhodoev, V., Francke, A., Ritter, B., Raschke, U., Nowaczyk, N., Schwamborn, G., Brigham-Grette, J., and Melles, M.: Pliocene to Pleistocene climate and environmental history of lake El'gygytgyn/NE Russia based on high-resolution inorganic geochemistry data, Clim. Past., in preparation, 2013.

Table 1. Information on drilling of sediments from cores 1A, 1B and 1C from ICDP Site 5011-1 in Lake El'gygytgyn. In core 1C sediments were first recoved from 42 to 50 m (shown in brackets) to patch up gaps in sediment recovery in cores 1A and 1B. After that drilling was continued at depth 100.0 m.

Drilling of lake sediments on ICDP Site 5011-1					
Core	Start (m)	End (m)	Drilled (m)	Recovered (m)	Recovery (%)
5011-1A	2.9	146.6	143.7	132.0	92
5011-1B	3.5	111.9	108.4	106.6	98
5011-1C	(42.0) 100.0	(51.0) 316.3	225.3	116.1	52

CPD
9, 5077–5122, 2013

Table 2. Information on magnetic parameters used to characterize mineral magnetic assemblages in catchment rocks, creek sediments and lake sediments from Lake El'gygytgyn and its catchment. CR = catchment rocks, CS = creek sediments and LS = lake sediments.

Parameter	Instrument	Unit	Explanation	Notes
Magnetic measurements				
Low-field volumetric magnetic susceptibility κ_{LF}(SI, $\times 10^{-6}$)	Kappabridge MFK1-A (AGICO)	Unitless	Used for estimation of concentration of magnetic minerals in uniform magnetic mineralogy. As an in-field parameter, κ_{LF} may be increased by paramagnetic minerals and superparamagnetic grains, which do not carry remanence. Essentially independent of magnetite grain size.	Measured from CR, CS and LS
Isothermal remanent magnetization, IRM	Either (1) for imprinting the desired field: impulse magnetizer (2G model 660) and for the measuring of the remanence: minispin spinner magnetometer (Molspin Ltd.) or (2) alternating field magnetometer MicroMag 2900 (Princeton Measurements Corp.)	$\mathrm{A\,m^{-1}}$	Magnitude of standalone IRM measurements relates to magnetite concentration and inversely to magnetite grain size. Observations of IRM of samples exposed to incrementally higher fields (acquisition of IRM, i.e. aIRM) bring forth information on magnetic mineralogy as a function of coercivity. Conventionally saturation IRM (SIRM) designates the IRM produced in the highest field adopted (1–2.5 Teslas). Magnitude of IRM is inversely dependent on magnetite grain size. Measurement of a remanence induced in a reversed direction after peak field (usually 10–20 % from peak field strength) allows estimating the easiness of remagnetization, which is interpreted in terms of magnetic mineralogy or grain size.	– CR and LS: aIRM measurements performed using option (1) with peak field 2500 mT and backfield 200 mT – For CS: aIRM measurements were performed using option (2) with peak field 2000 mT and backfield 300 mT.
Parameters related to determination of magnetic grain size				
– Saturation magnetization M_s – Saturation remanent magnetization M_{rs} – Coercive field B_c	Alternating field magnetometer Micromag 2900	$\mathrm{A\,m^{-1}}$	M_S is an in-field measure and describes magnetization in a saturating field. M_{SR} is the remanence left after switching off the field. B_C is an in-field measure and it states the field strength required to bring magnetization to zero after saturation. In particular, B_C reflects magnetite grain size. Measurement of a hysteresis loop allows the determination of M_s, M_{rs} and B_c.	Measured only from CS and LS
– Coercivity of remanence B_{cr}	Alternating field magnetometer Micromag 2900	mT	B_{cr} expresses the magnetic field strength required to demagnetize M_{sr} to zero remanence. B_{cr} reflects both magnetic mineralogy and grain size.	Measured only from CS and LS
Interparametric ratios				
SIRM/κ_{LF}		$\mathrm{kA\,m^{-1}}$	Sensitive to magnetic grain size in magnetite. Values vary inversely with magnetic grain size. As essentially a concentration dependent parameter, κ_{LF} is used for normalizing the concentration dependence of SIRM, leaving out information on grain size.	CR, CS and LS
S-ratio		Unitless	Ratio between two IRM measurements. Calculated here as $0.5 \cdot [1-(\mathrm{IRM@highest\ field}/\mathrm{IRM@back\text{-}field})]$. Allows estimating the easiness of remagnetization, which relates to magnetic mineralogy. Commonly interpreted as the ratio between magnetite and hematite in a sample, where value 1 (0) designates the only magnetic mineral present is magnetite (hematite).	CR, CS and LS
M_s/M_{sr}		Unitless	The ratio M_s/M_{sr} is inversely related to magnetite grain size. This ratio is used as a part of Day plot to characterize magnetite domain state.	CS and LS
B_c/B_{cr}		Unitless	The ratio B_c/B_{cr} is directly proportional to magnetite grain size. This ratio is used as a part of Day plot the characterize magnetite domain state.	CS and LS

CPD
9, 5077–5122, 2013

E. M. Haltia and N. R. Nowaczyk

Table 3. Selected magnetic parameters from catchment rocks, creek sediments and lake sediments. Mean value, (standard deviation) and [total range of values] are shown. See text for discussion.

Investigated material	Parameter/ratio κ_{LF}(SI 10^{-6})	SIRM (A m^{-1})	S-ratio	SIRM/κ_{LF}(kA m^{-1})	B_{cr}(mT)
Catchment rocks					
– Bedrock	10 749 (10 238) [365.26–30 960]	105.28 (69.73) [5.31–252.17]	0.95 (0.05) [0.79–0.99]	23.49 (25.85) [1.85–80.57]	n/a
– Colluvium	9498.0 (9874.5) [62.49–49 026]	157.55 (144.50) [1.29–843.50]	0.92 (0.15) [0.46–1.00]	25.00 (20.40) [0.69–98.46]	n/a
Creek sediments	3072.6 (1661.5) [1516.5–7906.7]	20.27 (7.12) [10.62–41.29]	0.98 (0.01) [0.96–0.99]	7.30 (2.19) [3.76–12.81]	32.28 (8.86) [20.27–50.09]
Lake sediments	2557.7 (2630.0) [124.60–17 590]	18.17 (15.61) [0.43–75.16]	0.98 (0.05) [0.57–0.99]	7.42 (1.80) [2.05–13.21]	23.40 (4.99) [18.60–44.57]

CPD
9, 5077–5122, 2013

Table 4. Magnetostratigraphic tie-points, their depth in composite record from Site 5011-1 and their age (Ma) from LR04, except for the ages of Cobb Mountain and Réunion cryptochrons, which are from Ogg and Smith (2004). Ages for Intra-Jaramillo and Olduvai precursor events are derived from tuning with respect to LR04 stack (Nowaczyk et al., 2013).

Polarity chron, subchron, cryptochron, event	Composite depth (m)	Age (Ma)
Brunhes/Matuyama	31.710	0.780
Jaramillo (t)	41.530	0.991
Intra-Jaramillo (t)	42.330	1.0142
Intra-Jaramillo (b)	42.480	1.0192
Jaramillo (b)	44.110	1.073
Cobb Mountain (t)	47.800	1.175
Cobb Mountain (b)	48.125	1.185
Olduvai (t)	79.480	1.781
Olduvai (b)	88.425	1.968
Olduvai precursor (t)	89.020	1.978
Olduvai precursor (b)	89.190	1.981
Reunion (t)	100.630	2.128
Reunion (b)	101.150	2.148
Matuyama/Gauss	123.550	2.608
Kaena (t)	160.650[a]	3.045
Kaena (b)	163.500	3.127
Mammoth (t)	172.300	3.210
Mammoth (b)	197.400[b]	3.319
Impact	319.700	3.580

[a] Low data quality prevents accurate determination of termination of Kaena subchron.
[b] The depth value for the base of Mammoth subchron represents a minimum value because of a gap in sediment recovery. Impact age is from data presented by Layer (2000).

CPD
9, 5077–5122, 2013

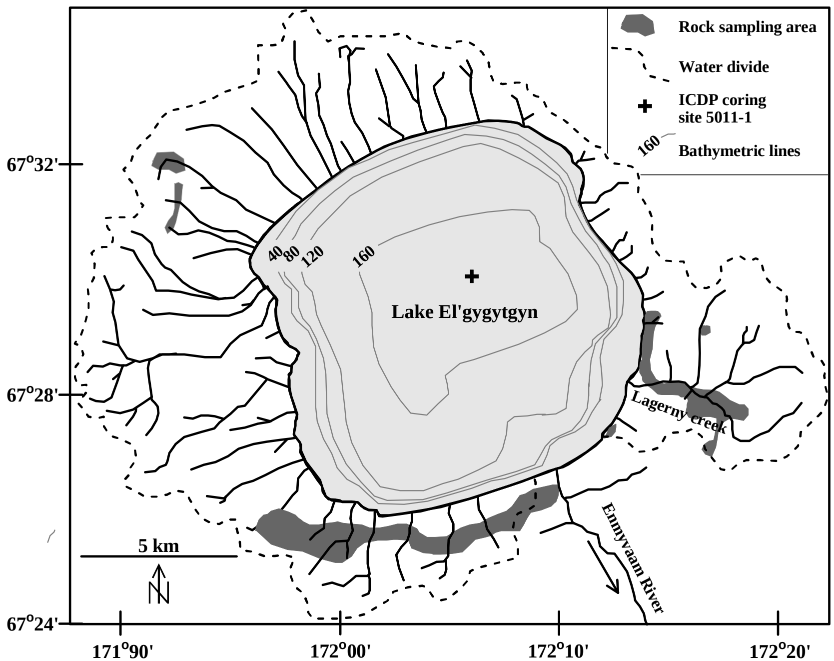

Fig. 1. Schematic map of Lake El'gygytgyn and its catchment. Largest creeks are marked in the map by thick solid lines. The location of ICDP Site 5011-1, in the flat central part of the bowl-shaped lake floor, is marked by a cross. The rim of the impact crater mostly follows the border of the lake's catchment (dashed line).

CPD
9, 5077–5122, 2013

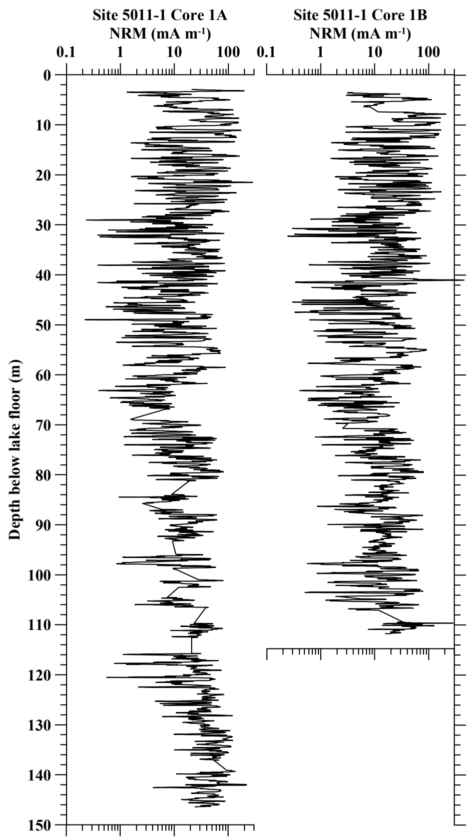

Fig. 2. Down-core variations in the intensity of the natural remanent magnetization (NRM) in cores 1A and 1B.

CPD
9, 5077–5122, 2013

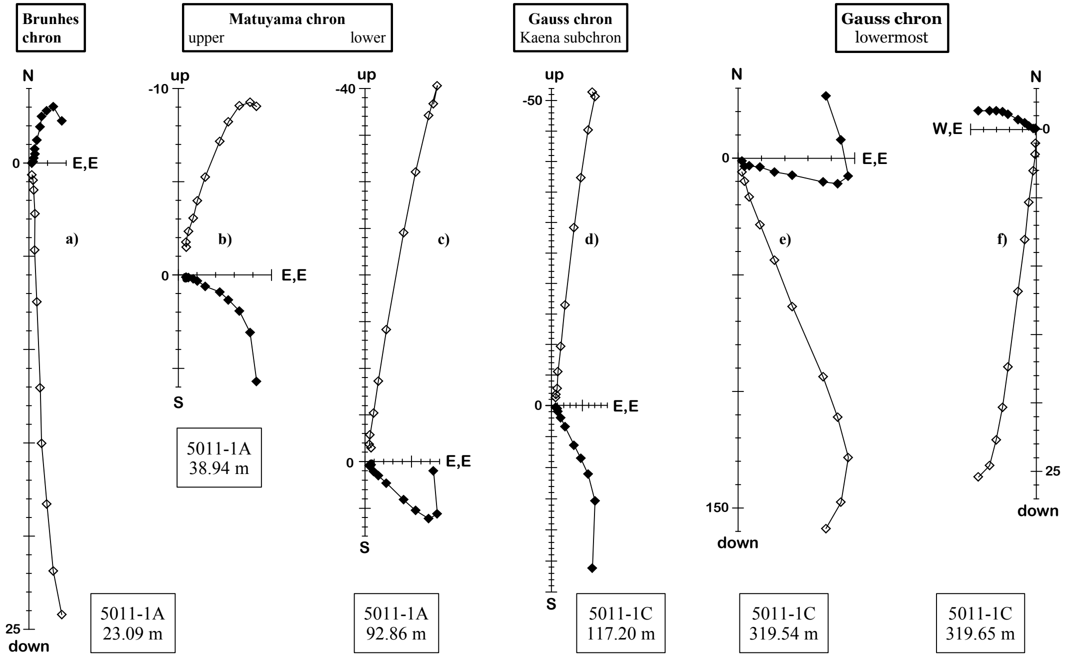

Fig. 3. Representative vector endpoint diagrams obtained from progressive alternating field demagnetization of natural remanent magnetization of sediments from cores 1A **(a–c)** and 1C **(d–f)** from Lake El'gygytgyn. Samples show high directional stability. Solid (open) diamonds indicate projection to the horizontal (vertical) plane. Axes are individually scaled from graph to graph with units in mA m^{-1}.

CPD
9, 5077–5122, 2013

Magnetostratigraphy of sediments from Lake El'gygytgyn

E. M. Haltia and N. R. Nowaczyk

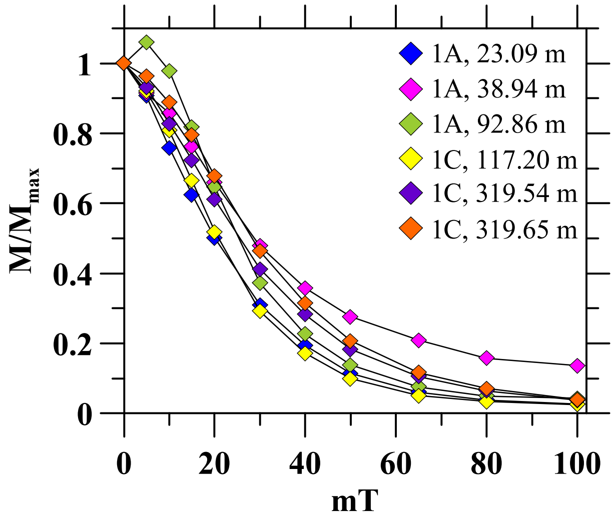

Fig. 4. Curves of normalized NRM intensity vs. peak alternating field demagnetization steps from 0 to 100 mT. Samples are the same as in Fig. 3. Smoothly reducing remanence is indicative of low-coercivity magnetic components dominating the remanence in these samples.

CPD
9, 5077–5122, 2013

E. M. Haltia and N. R. Nowaczyk

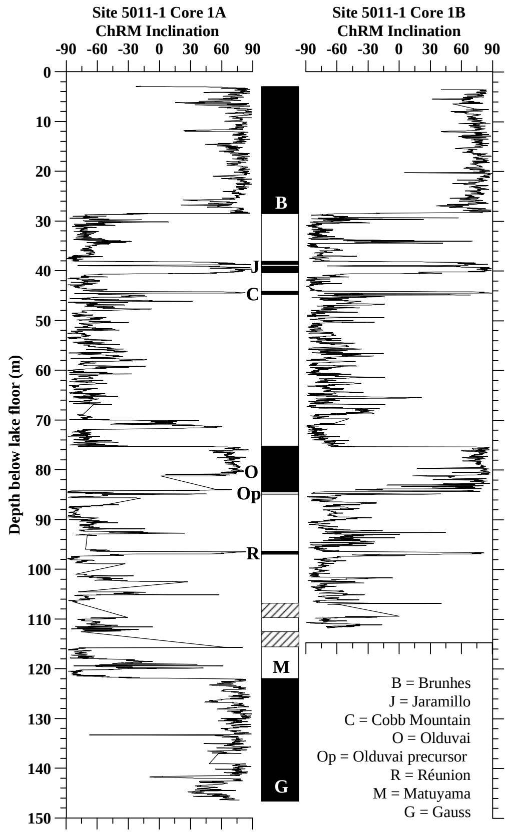

Fig. 5. Down-core variations in the inclinations of the characteristic remanent magnetization (ChRM) from cores 5011-1A and 1B. In the polarity column, black (white) (gray) denotes normal (reversed) (unclear) polarity. Letters refer to polarity chrons, subchrons and cryptochrons, and their meaning is explained in the legend.

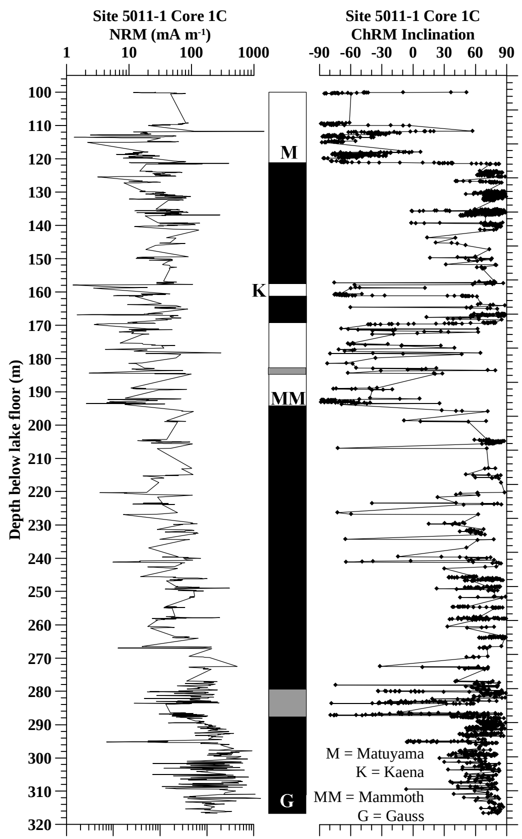

Fig. 6. Down-core variations in the ChRM inclination from core 5011-1C. In the polarity column, black (white) (gray) denotes normal (reversed) (unclear) polarity. Letters refer to polarity chrons, subchrons and cryptochrons, and their meaning is explained in the legend.

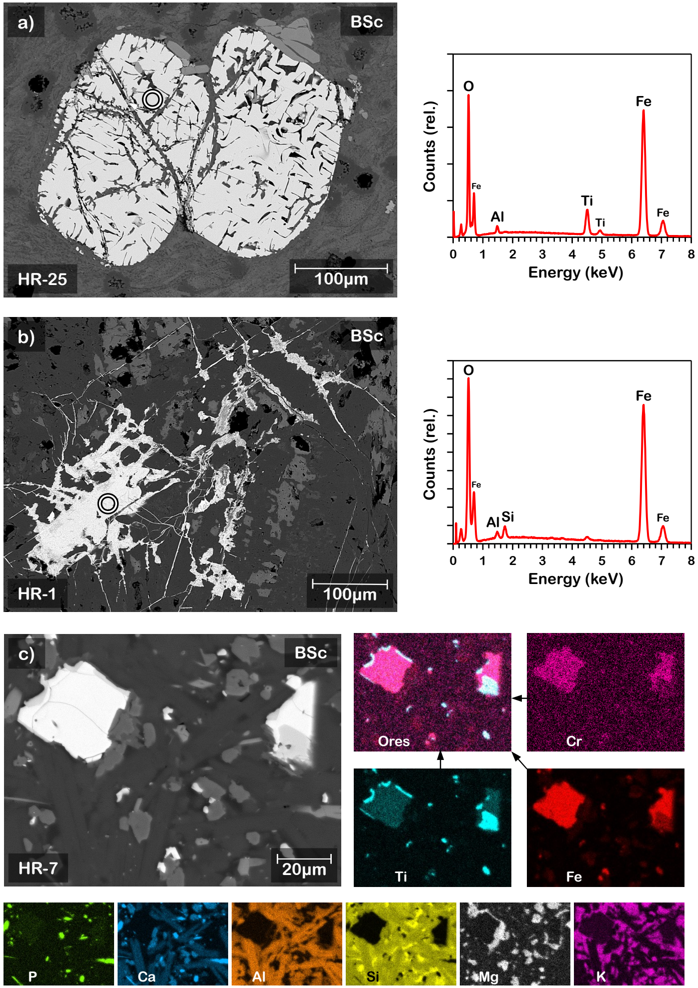

CPD
9, 5077–5122, 2013

Magnetostratigraphy of sediments from Lake El'gygytgyn

E. M. Haltia and N. R. Nowaczyk

Title Page
Abstract | Introduction
Conclusions | References
Tables | Figures
Back | Close
Full Screen / Esc
Printer-friendly Version
Interactive Discussion

Fig. 7. Scanning electron microscope (SEM) analyses of polished sections from selected catchment rock samples: **(a)** SEM image and EDS analysis of a large titano-magnetite grain, $Fe_{3-x}Ti_xO_4$ ($0 \leq x \leq 1$), in a rhyolitic sample from the distal south-eastern catchment. Visible (shrinkage) cracks might be due to in-situ low-temperature oxidation (maghemitization). **(b)** SEM image and EDS analysis of an iron oxide, probably hematite, in a rhyolitic sample from the eastern shore line, **(c)** SEM image and corresponding elemental mapping of major elements in a basaltic-andesitic sample from the distal eastern catchment. Ore grains (superimposed Fe-, Ti-, Cr-mapping) show intergrowth of titano-magnetite and Cr-bearing magnetite, $FeFe_{2-x},Cr_xO_4$ ($0 \leq x \leq 2$). Bright patches both in the P- and Ca-mappings point to the presence of apatite, $Ca_5(Cl,F,OH)(PO_4)_3$, whereas mappings of Ca, Al, Si, Mg, and K together reflect the distributions of various silicates. The circles in **(a)** and **(b)** mark the locations of EDS analyses. EDS – energy dispersive X-ray spectroscopy, BSc – back scatter electrons.

CPD
9, 5077–5122, 2013

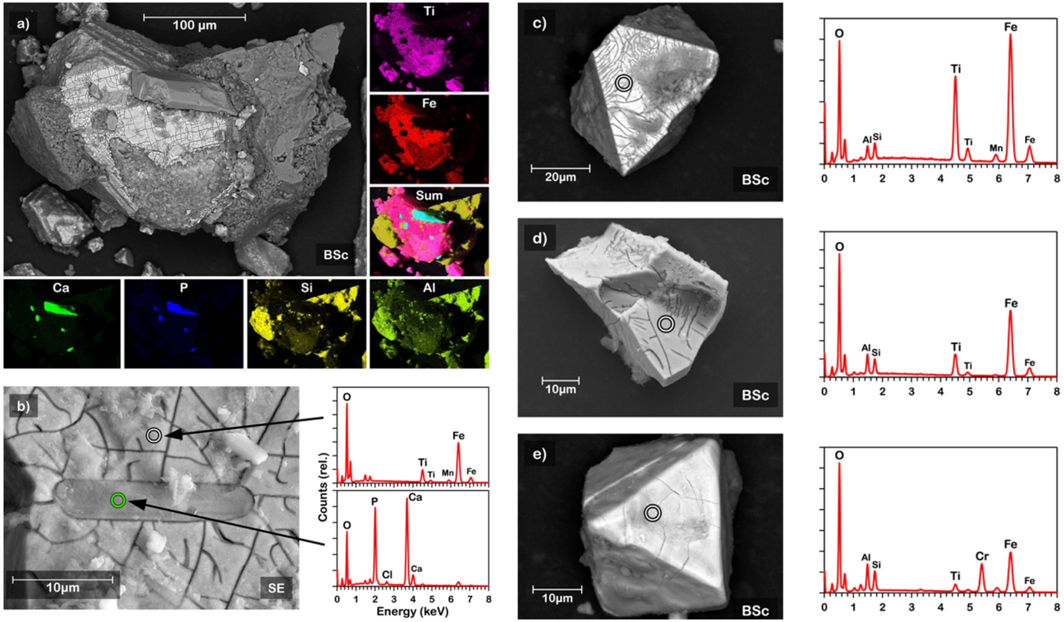

Fig. 8. Scanning electron microscope (SEM) analyses of magnetic extracts from creek sediments from the northwestern shore of El'gygytgyn: **(a)** SEM image and elemental mapping of a large (~ 400 µm) titano-magnetite grain, $Fe_{3-x}Ti_xO_4$ ($0 \leq x \leq 1$), represented by the Fe- and Ti-mappings. The Ti-magnetite is still encrusted by minerals of the host rock, where bright patches in the P- and Ca-mapping indicate the presence of apatite, $Ca_5(Cl,F,OH)(PO_4)_3$, whereas mappings of Al and Si reflect the distributions of silicates. **(b)** A close-up of another Ti-magnetite with apatite inclusion, together with associated EDS analyses. **(c)** Idiomorphic and **(d)** irregular Ti-magnetite grain. **(e)** Idiomorphic Cr-bearing magnetite, $FeFe_{2-x},Cr_xO_4$ ($0 \leq x \leq 2$). More or less distinctively visible shrinkage cracks in all grains indicate low-temperature oxidation (maghemitization). The circles from **(b)** to **(e)** mark the locations of EDS analyses. EDS – energy dispersive X-ray spectroscopy, BSc – back scatter electrons, SE – secondary electrons.

CPD
9, 5077–5122, 2013

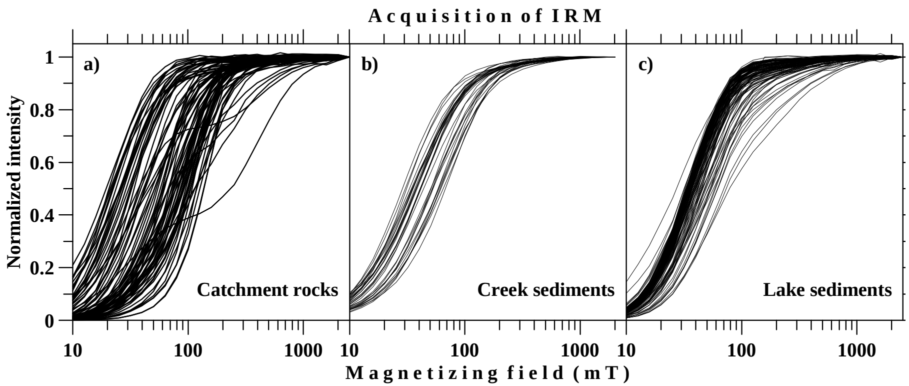

Fig. 9. Normalized acquisition of isothermal remanent magnetization (IRM) with respect to applied magnetic field strength in different sample types. **(a)** Catchment rocks gain remanence rapidly in low fields indicating the presence of multi-domain Ti-magnetite. **(b)** Creek sediments appear more homogenous in their grain size and mineralogy, and most samples are saturated by magnetic field 200 mT in strength, which is typical of (Ti-) magnetite. **(c)** Similar to catchment rocks, some lake sediment samples indicate the presence of high-coercive magnetic minerals. Most of the samples are dominated by low-coercivity Ti-magnetite, as demonstrated by (near) saturation in fields < 200 mT.

CPD
9, 5077–5122, 2013

E. M. Haltia and N. R. Nowaczyk

Title Page
Abstract | Introduction
Conclusions | References
Tables | Figures
◀I | ▶I
◀ | ▶
Back | Close
Full Screen / Esc
Printer-friendly Version
Interactive Discussion

CPD
9, 5077–5122, 2013

Magnetostratigraphy of sediments from Lake El'gygytgyn

E. M. Haltia and N. R. Nowaczyk

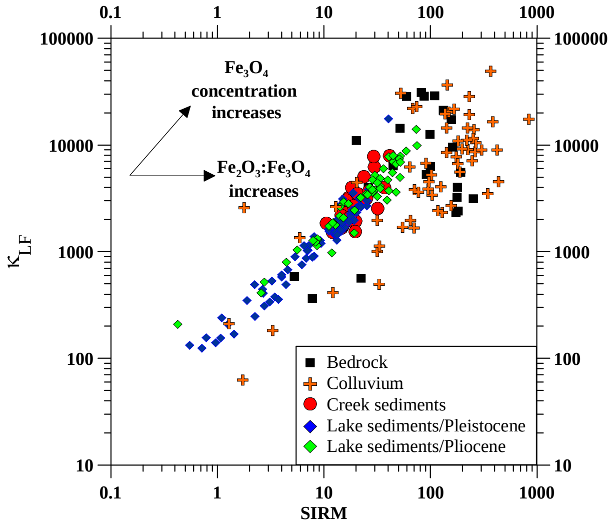

Fig. 10. Biplot of magnetic susceptibility (κ_{LF}) vs. saturation remanent magnetization (SIRM). Deviations from a linear relationship between the two parameters in different sample types indicate variation in the proportions of the constituting magnetic minerals in rock/sediment magnetic assemblages. Catchment rocks, including colluvium and bedrock, show widely varying magnetic properties, whereas data from creek sediments are notably clustered. In contrast to catchment rocks, lake sediments indicate a linear relationship between the two magnetic parameters. This suggests a homogenous magnetic assemblage in the sediment column.

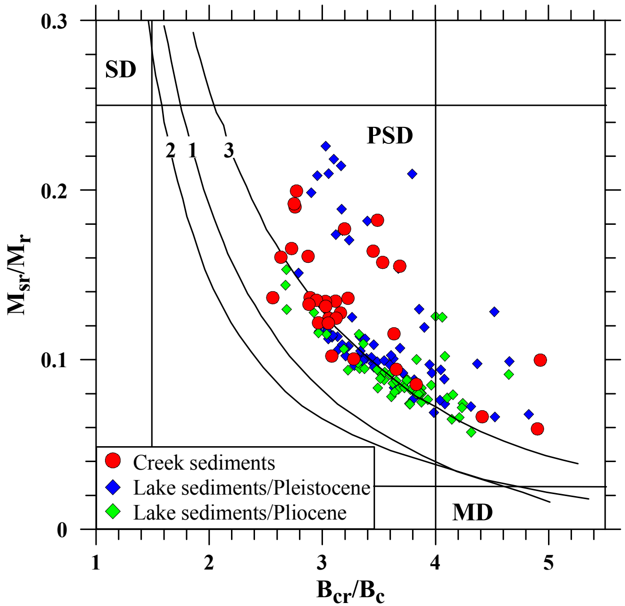

Fig. 11. Modified Day plot (Day et al., 1977) of magnetic hysteresis data obtained from material from Lake El'gygytgyn and its catchment. Symbols refer to the the same material as listed in Fig. 10. Experimental mixing lines 1 and 2 refer to Dunlop (2002), and line 3 refers to work by Parry (1980). Ratios calculated using data from hysteresis analyses and measurement of coercivity of remanence are indicative of magnetic domain status in Ti-magnetite. The majority of samples plot near mixing line 3, which suggests a PSD to MD domain state of the analysed samples. In particular Pleistocene age lake sediment samples and creek sediments plot right from the theoretical mixing lines. This is probably due to maghemitization of Ti-magnetites.

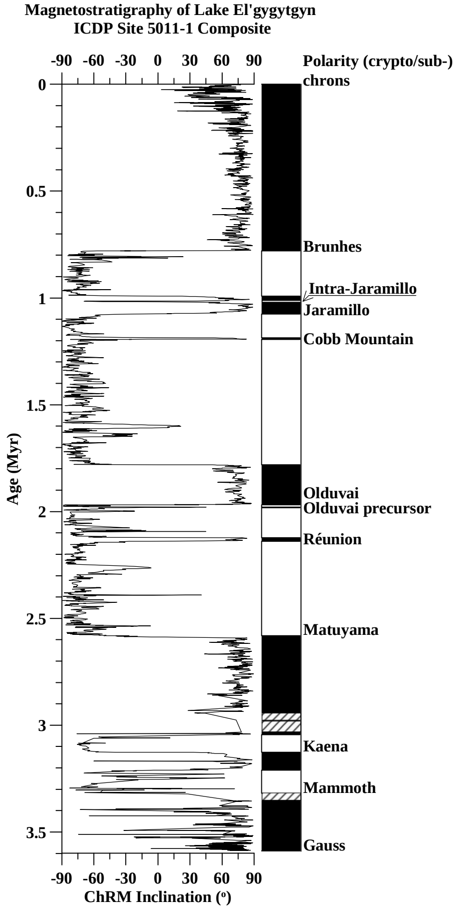

Fig. 12. Composite record of ChRM inclinations from ICDP Site 5011-1 in Lake El'gygytgyn. In the polarity column, black (white) (hatched) denotes normal (reversed) (missing) polarity.

CPD
9, 5077–5122, 2013

Magnetostratigraphy of sediments from Lake El'gygytgyn

E. M. Haltia and N. R. Nowaczyk

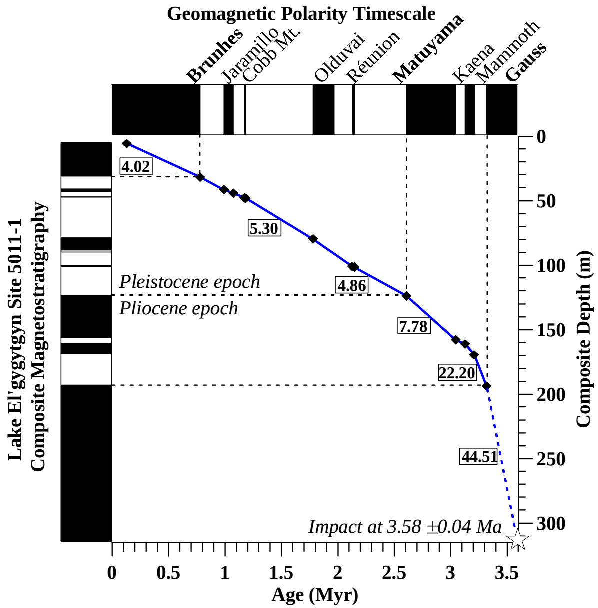

Fig. 13. Age-depth curve of the composite record (in blue) based on stratigraphical tie-points (black diamonds) provided by the magnetostratigraphy. Age of the impact (Layer, 2000) denoted with a star forms an additional chronological tie point. Numbers in boxes refer to sedimentation rates (cm kyr^{-1}) in different intervals of the composite record.

CPD
9, 5077–5122, 2013

Magnetostratigraphy of sediments from Lake El'gygytgyn

E. M. Haltia and N. R. Nowaczyk

Title Page
Abstract Introduction
Conclusions References
Tables Figures
Back Close
Full Screen / Esc
Printer-friendly Version
Interactive Discussion